
Transport Network Resilience Following a Natural Disaster

Elie Attias * Julie-Alexia Dias *

Abstract

In this paper, we propose a method to simulate the effects of natural disasters on transport networks, testing the resilience of such network using percolation theory. The edges of the network represent roads (i.e. highways, primary or secondary roads, trails) while the vertices represent their intersection. The probability model according to which roads are susceptible to breakage are determined based on their proximity to the source of the earthquake and the earthquake's features. Following percolation-like damage simulation, in which the network is sequentially susceptible to breakage, the final connectedness of the graph is analyzed. In our application, the Turkish road network was exposed to a series of earthquakes from Feb 2nd 2023 to Feb 10th 2023, located close to the Turkish-Syrian border, by the East Anatolian Fault. We found that these earthquakes resulted in a systemic divide in the graph, separating West and East Turkey. Moreover, we were able to identify recurring isolated components, which could help identify the optimal locations for emergency resource centers in future similar natural disasters.

1. Introduction

Natural disasters, such as earthquakes, can cause widespread damage and pose threats to human lives, infrastructure, and economies. It is therefore paramount to better understand seismic events and accurately forecast their potential impacts on built infrastructure, human lives, and the environment. Such predictive capabilities enhance early warning systems, allowing authorities to implement timely evacuation plans, allocate resources efficiently, and minimize the loss of life and property. Recently, a series of earthquakes hit the Turkish-Syrian border, resulting in significant road damages and casualties.

Turkey is located on top of two main fault zones: the East and North Anatolian which makes it one of the most seismically active regions on the world. On February 6, 2023, at 4:17 a.m. local time, a 7.8 magnitude earthquake rocked southeast Turkey near the Syrian border. The initial quake

struck at a depth of 11 miles (17.9 km) near Nurdagi in Gaziantep province. Since the first quake, aftershocks numbering in the thousands have rumbled across the region, according to the United Nations Office for the Coordination of Humanitarian Affairs (OCHA). (1). During this period, the Turkish government, along with local authorities and response teams, swiftly mobilized to provide relief efforts and support to affected communities. The response included deploying search and rescue teams, establishing temporary shelters, providing medical assistance, and distributing aid to those in need. These efforts aimed to mitigate the impact of the earthquakes and aid in the recovery and reconstruction process.

While the recent Turkish earthquakes have been devastating, they have also highlighted the significance of earthquake monitoring, preparedness, and response. The location of emergency resources can be optimized to minimize casualties and ensure access to basic necessities such as food, water and emergency shelter to civilians. In order to identify these optimal locations, the impact of an earthquake on the road network's resilience can be analyzed by assessing the vulnerability of individual road segments to seismic forces. Multiple methods to study network resilience have been studied, including inclusion-exclusion algorithms (Sun et al., 2012) percolation theory (Li et al., 2015) and other probabilistic models (Ball et al., 1995). In this paper, we use principles of percolation theory to simulate road breakage following a series of earthquakes and study the resulting graph's connectedness.

2. Literature Review

Varying scales exist to measure the impact of an earthquake on its environment. One widely used scale is the moment magnitude scale (Mw), which quantifies the energy released by an earthquake. The Mw scale provides an objective measure of the earthquake's strength and helps in comparing earthquakes of different magnitudes. Another commonly used scale is the Modified Mercalli Intensity (MMI) scale, which assesses the earthquake's effects on the ground and structures. The MMI scale describes the observed shaking and resulting damage at specific locations, providing valuable information on the impact on infrastructure and communities. However, either scales were found to be inad-

equate to clearly define the road damage (Anbazhagan et al., 2012). Depending on the earthquake's magnitude, focal depth and location, the impact on the nearby infrastructure may vary. Additional factors such as the road's altitude may be beneficial to better predict its breakage probability.

(Schaeffer, 2007) gives an overview of various methods used to identify clusters within graphs. However, in this case we want to identify recurring isolated components over multiple simulations. In this context, hierarchical clustering based on isolated component membership allows to identify these isolated clusters. Grid-based methods as described in (Murtagh & Contreras, 2012) can be used for geographical data and have been used in various applications, such as image segmentation, spatial data analysis, and data mining. Upon forming the linkage matrix based on the correlation matrix generated from the percolated graph, different inconsistency thresholds can be selected to vary the size of the resulting isolated clusters.

(Kilanitis & Sextos, 2019) explored the effects of earthquake-induced bridge damage and time-varying traffic demand on the resilience of road networks. They found that the resilience of a road network is significantly influenced by the location and severity of bridge damage resulting from earthquakes. Bridges serve as critical network components, and their failure can lead to significant disruptions and cascading effects on the overall network performance. Moreover, in (Sextos et al., 2017) the authors emphasize the significance of network connectivity and redundancy in enhancing resilience. A well-connected network with multiple alternative routes allows for rerouting and detouring traffic in the event of road closures due to earthquake damage. Redundancy in the network helps in maintaining accessibility and reducing disruptions.

3. Model

Our model is comprised of three steps: generate breakage probabilities based on edge intensities, simulate percolation on graph sequentially (earthquake by earthquake) and identify recurring isolated components.

3.1. Edge breakage probabilities

We assume that the probability of an edge breaking (and therefore being removed from the graph) is proportional to its intensity exposure during the earthquake. Moreover, the intensity is a function of the earthquake's magnitude and depth and the edge's hypodistance (i.e. the distance between the edge and the earthquake's hypocenter). In order to define this relationship, we use two of the recent earthquakes with the richest data to derive our constants, namely the [Pazarcik earthquake](#) (2023-02-06 01:17:34 (UTC), magnitude 7.8, depth 10.0 km) and the [Uzunba earthquake](#) (2023-02-20

17:04:29 (UTC), magnitude 6.3, depth 16.0 km). The maximum intensity varies by earthquake magnitude while the decrease in intensity is a function of hypodistance. A linear regression is run on both earthquakes as such

$$Int_P = a_P + b_P \log_{10}(d_{ij})$$

for the Pazarcik earthquake, and

$$Int_U = a_U + b_U \log_{10}(d_{ij})$$

for the Uzunba earthquake, where the hypodistance of edge i from earthquake j is

$$d_{ij}^2 = ((x_i - l_{oj}) * 111)^2 + ((y_i - l_{aj}) * 111)^2 + (q_j + a_i)^2$$

with x_i being the road's center longitude coordinate and y_i being the road's center latitude coordinate, a_i being the altitude in km, for edge i , l_{oj} being the longitude coordinate and l_{aj} being the latitude coordinate and q_j being the depth in km, for earthquake j . A correction factor of 111 is employed to transform a change in geographical coordinates to a change in distance. A line is fitted through (m_P, a_P) and (m_U, a_U) , where m_j is the magnitude on the Richter scale of earthquake j to define the linear relation between the intercept coefficient and earthquake magnitude.

The breakage probability of edge i from earthquake j can then be formulated as

$$p_{ij} = \sigma_a((\alpha \times M_j + \beta) + (\gamma + \delta M_j) \times d_{ij})$$

where $\sigma_k(x) = (1 + e^{k-x})^{-1}$, $a = 9$, $\alpha = 2.79$, $\beta = -7.616$, $\gamma = 1.974$ and $\delta = -0.78$.

These intensities are converted into a breakage probability via a shifted sigmoid. Here a k of 9 is chosen, to reflect the likelihood of road breakage following the EMS-98 scale. Any road with intensity less than 9 should have a probability of breakage < 0.5 to reflect the low impact of such exposure.

3.2. Sequential percolation-like simulation

We begin with a fully-connected graph, representing the transport network. For each earthquake j , the event indicating if edge i gets removed follows a Bernoulli distribution of parameter p_{ij} . The graph is sequentially subject to breakage for each earthquake and the resulting percolated graph can be analyzed.

3.3. Identification of recurring isolated components

For a single simulation, we can identify the connected components of generated percolated graphs from their incidence matrix, as shown in 5. Running multiple simulations, we can generate a global frequency matrix F , where F_{ij} represents the frequency at which two nodes are measured to be in

the same connected component within the percolated graph. Intuitively, nodes with large correlations are more likely to belong to the same isolated component after a simulation. The structure of the correlation matrix can be examined to find distinct patterns which reflect the connectedness of the percolated graph where, for example, clear independent correlated blocks indicate isolated components.

The frequency matrix F is then converted to a distance matrix using Euclidean distance (`scipy.spatial`) which is passed to a hierarchical clustering algorithm (`scipy.cluster`). The inconsistency threshold is set to obtain a reasonable of clusters and the resulting clusters correspond to the recurring isolated components. A city/village within the isolated component is then defined as a potential emergency resource location.

4. Methodology and Results

4.1. Data Collection

The data we used throughout this project is fourfold. First we collected geographical information on the Turkish road network through ([Humanitarian Data Exchange](#)). Second, we obtained road altitudes from the NASA Shuttle Radar Topography Mission Global 1 arc second V003 ([NASA Disasters Mapping Portal](#)). Third, we collected data on the location of the most recent earthquakes from the USGS Earthquakes Hazard Program ([USG](#)). Fourth, we collected the location and population density of Turkish cities at ([SimpleMaps](#)).

4.2. Turkish Transport Network and Earthquake data

The collected Turkish transport network consists of 53,414 roads that span the whole country as shown in Figure 1. The seismic dataset analyzed in this study comprises a total of 244 earthquakes, occurring between the 3rd and 10th of February 2023, with their epicenters originating from the East Anatolian Fault in Turkey. The geographical distribution of these earthquakes is illustrated in Figure 1. Notably, the majority of seismic events took place on the 6th of February 2023. A detailed summary of the earthquake characteristics is presented in Table 1. Notably, one earthquake recorded a magnitude of 7.8, resulting in substantial damage.

Table 1. Earthquake Characteristics Summary

Day	# Earthquakes	Maximum Magnitude	Mean Magnitude
02/03	1	4.2	4.2
02/06	164	7.8	4.58
02/07	44	5.5	4.47
02/08	21	5.4	4.42
02/09	13	4.6	4.28
02/10	1	4.3	4.3

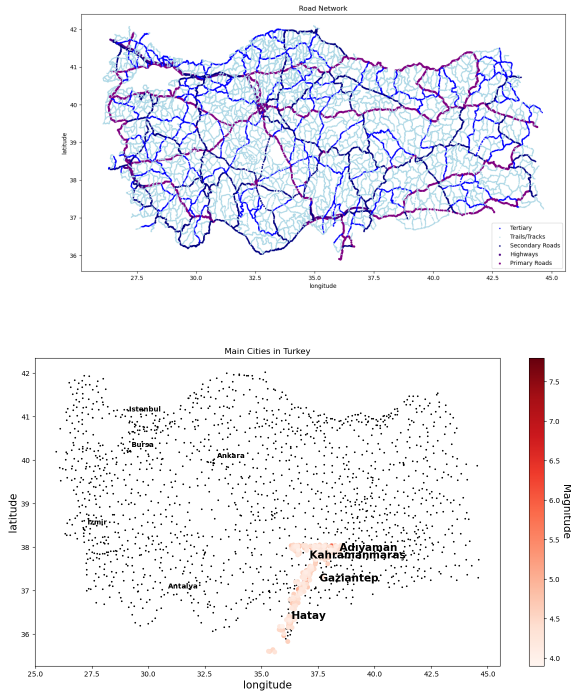


Figure 1. Turkish Road Network and Earthquake epicenters
description of the figures

4.3. Prior Analysis of turkey's Road Network

In order to assess the importance of each road in the Turkish transportation network, we computed the betweenness centrality of every node in the graph. We recall that the latter is a measure of centrality in a graph that is based on shortest paths. Indeed, for every pair of vertices in a connected graph, there exists at least one shortest path between the vertices such that either the number of edges that the path passes through is minimized. This measure is computed as follows: $g(v) = \sum_{s \neq v \neq t} \frac{\sigma_{st}(v)}{\sigma_{st}}$ where σ_{st} is the total number of shortest paths from node s to node t and $\sigma_{st}(v)$ is the number of those paths that pass through v . Mapping the centrality of each node across the Turkish Road Network yields Figure 2. We recover that the most central roads in the Turkish road network are along highways showing that the Turkish highways are efficiently located. Additionally, this shows that if earthquakes damage these roads, the Turkish road network will get dramatically slowed down. We note that this analysis does not take into account other external parameters such as speed limitations, traffic or population density and relies purely on the spatial location of the roads.

4.4. Simulating Earthquakes

The original fully-connected Turkish road network comprises of 51859 vertices and 53414 edges, again representing roads and either their intersection or a certain point

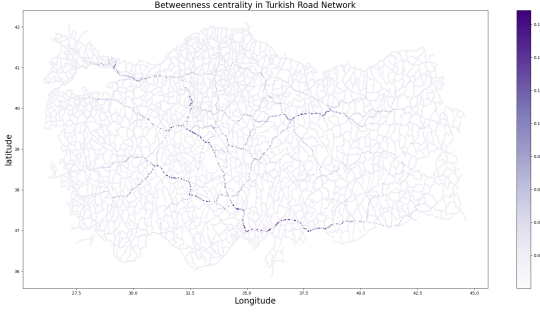


Figure 2. Betweenness Centrality of nodes in Turkish Road Network The betweenness centrality of every node in the graph is visualised in this figure. The nodes with the highest centrality overlap with the locations of highways meaning that highways are efficiently located, and that damaging these roads would substantially slow down the Turkish transportation network.

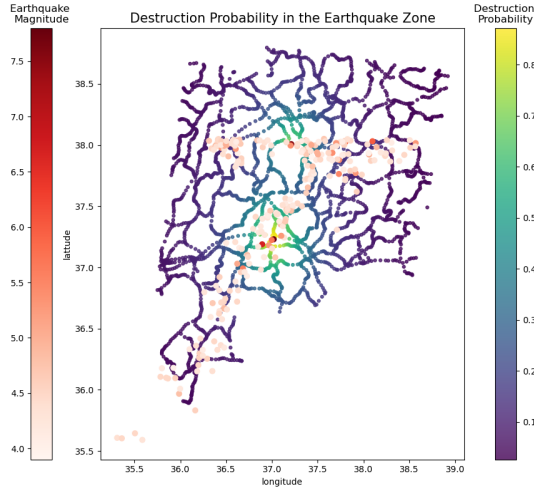


Figure 3. Destruction Probability In Earthquake Region The largest destruction probabilities overlap with the locations of the earthquakes with the largest magnitude.

within a road. The earthquakes are sequentially simulated, according to their timeline. Each edge i for earthquake j will be subject to breakage according to a Bernoulli trial with probability p_{ij} as defined above. The breakage probability for a subregion of Turkey covering earthquakes from Feb 2nd to Feb 10th 2023 is shown in Figure 4. The initially fully-connected graph is therefore percolated earthquake by earthquake and the final percolated graph is kept for analysis.

4.5. Degree Distribution Evolution in Key Regions

In order to assess the influence of the earthquakes on the interconnectedness of cities, we conducted an analysis on the degree distributions of cities that were identified as be-

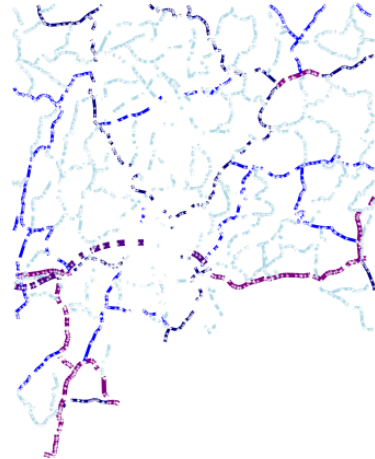


Figure 4. Broken Roads after all earthquakes Roads relatively close to the most devastating earthquakes are wiped out whereas further surrounding roads are more sparsely removed

ing significantly impacted by these seismic events. The examination focused on the changes observed in the road network surrounding Gaziantep both before and after the earthquakes, as well as the sequential degree distributions of the network nodes. Figure 6 provides visual representations of these findings.

4.6. Emergence of Isolated Components

In order to determine the potential areas in Turkey that may experience isolation following a series of earthquakes, we employed earthquake simulations and conducted an analysis of the resultant isolated connected components. The findings are illustrated in Figure 5. However, due to the stochastic nature of the simulations, the resulting connected components varied depending on the chosen seed. Therefore, we repeated the experiments across 100 seeds and recorded a binary variable in an $n \times n$ matrix, indicating whether nodes i and j were part of the same component, where $n = 51,859$ represents the number of nodes. We note that checking if a node is present in a connected component is equivalent to checking if the adjacent edge is in the connected component of edges meaning that such analysis over nodes extends to edges. We finally get an $100 \times n \times n$ tensor which we collapsed to an $n \times n$ matrix by taking the mean through the first dimension yielding a two dimensional matrix F matrix is symmetric with 1 across the diagonal. This is shown in figure 7.

The correlation matrices shown in 7 provide insights on the presence of 3 systems inside our graph. Specifically,

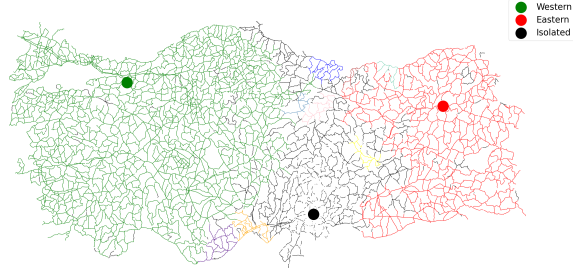


Figure 5. Resulting Road Network Components after simulating Earthquakes Following the simulations, four distinct systems emerge, namely the Western component, the Eastern component, medium-sized components, and a zone neighboring earthquakes, which comprises numerous nodes that are almost isolated. Among these systems, the medium-sized nodes are of particular importance and should be prioritized for the establishment of emergency centers

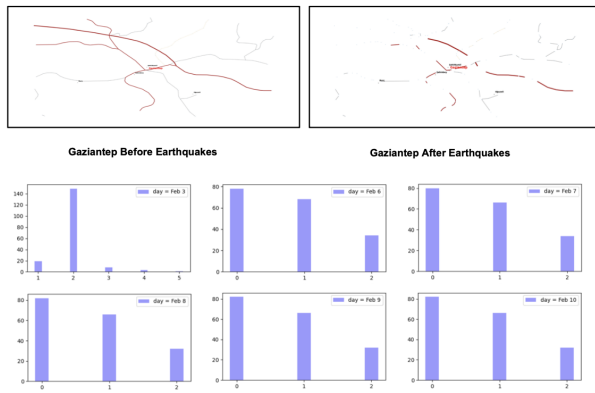


Figure 6. Resulting Road Network Components after simulating Earthquakes Initially, most nodes are connected to two roads, but the series of earthquakes on February 6th shifted this distribution and created various nodes of degree 0, dramatically the number of connected roads : from approximately 245 to 30.

attention is directed to the bottom right figure, where the rightmost square represents highly interconnected nodes, that are highly correlate to the Western node - labeled in 5. This suggests that these nodes form what we denote as the Western component. This component is the largest of all as suggested by the difference in side length of the squares. Conversely, the leftmost square represents a component of highly inter-correlated nodes that exhibit low correlation with the Western node. This suggests that these nodes are part of an Eastern component, situated considerably distant from the West. Additionally, the leftmost diagonal of the matrix comprises a set of nodes that demonstrate low correlation with one another, indicating their lack of cohesive integration. Instead, they form isolated nodes within the graph. Based on these findings, it can be inferred that these

Ordered Correlation Matrices Across the Graph

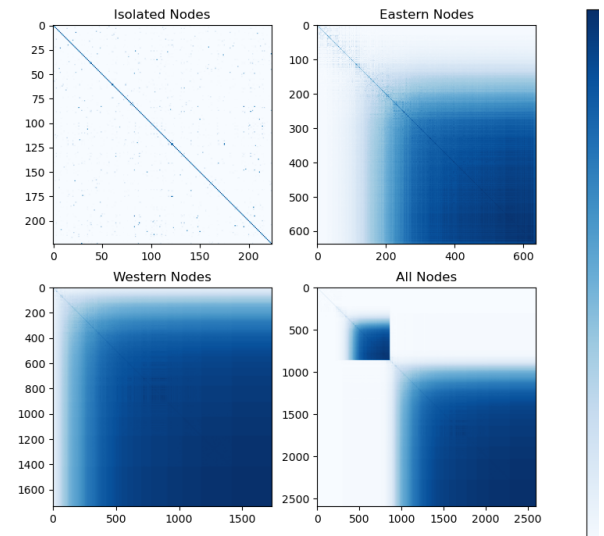


Figure 7. Resulting Correlation Matrices To construct the matrix located in the lower right corner, a node within the Western connected component was selected as a reference point. Subsequently, the correlation between this chosen node and all other nodes in the graph was computed and arranged in ascending order of correlation from left to right. Figure 5 provides the designated position of this node. Notably, for computational efficiency, only 0.25% of all correlations are displayed; however, including all nodes yields the same observed trend. The top left matrix pertains to isolated nodes, exhibiting no correlation with other nodes. The top right matrix represents the Eastern component, while the lower left matrix represents the Western component, encompassing the node within the Western connected component. The three correlation matrices, positioned in the top left, top right, and lower left respectively, are combined to form the final matrix in the lower right hence giving the reader a global picture of the graph's inter connectivity.

isolated nodes correspond to edges located near the Eastern Anatolian fault.

4.7. Systematic Identification of Isolated Components

The $n \times n$ frequency matrix \mathbf{F} is converted into a distance matrix taking the Euclidean distance i.e. the 2-norm. This distance matrix is then passed into a hierarchical clustering algorithm where the inconsistency threshold is set to achieve a number of clusters of ≈ 100 . Indeed isolated, or quasi-isolated nodes in the main damage region will tend to cluster together as they all have similar distances to other nodes. Moreover, given our simulations, the average number of connected components on the percolated graph is ≈ 2000 with a great majority of these connected components comprising of the isolated nodes in the damage region.

Similar to the correlation matrices previously discussed,

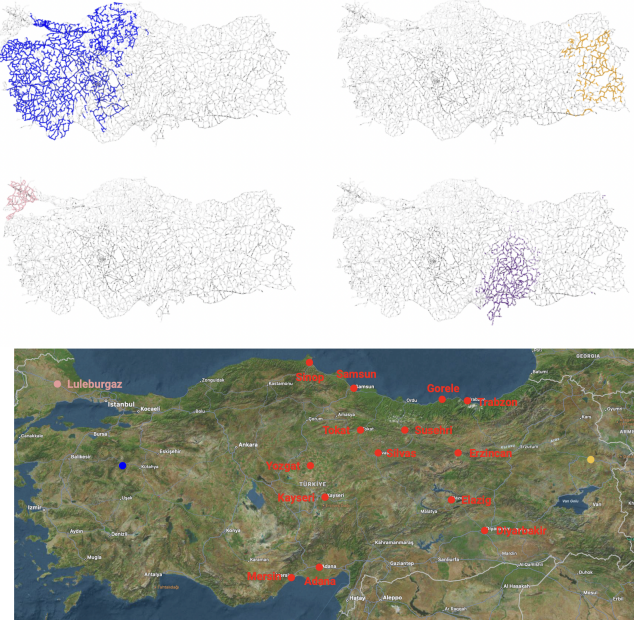


Figure 8. Identification of isolated components and Suggested Emergency centers The application of hierarchical clustering on inter-node correlations allows us to identify a subsets of nodes that are highly prone to forming a connected component following successive earthquakes. The visualization above displays four such zones, which signify areas at risk of isolation due to the lack of connecting roads with other components. By computing the edge betweenness centrality within each component, we can pinpoint edges that bear the highest traffic. These edges are selected as potential sites for emergency centers, minimizing the distance between the centers and zones requiring assistance.

the analysis of the resulting isolated components reveals two prominent recurring clusters corresponding to East and West Turkey, highlighted in yellow and blue respectively in Figure 7. Additionally, a distinct isolated component appears as a zone to the west of Istanbul, represented by the color pink. Lastly, as anticipated, the collection of isolated or quasi-isolated nodes conglomerates as one large isolated component. However, due to the extensive damage inflicted upon the majority of roads, making them impassable, the identification of an optimal location for an emergency center becomes unfeasible in this scenario.

5. Discussion

One of the primary contributions of our project is the introduction of a systematic methodology to identify zones that are most susceptible to isolation following a series of earthquakes. In the context of Turkey, our analysis revealed a number of isolated components that are at risk of being cut off following a series of earthquakes along the Eastern Anatolian fault. This identification process enabled us to propose optimal locations for emergency centers based on

graph theory principles, ensuring comprehensive coverage and mitigating the risk of leaving any zones helpless in the aftermath of earthquakes.

Moving forward, there are several crucial next steps for this project. Firstly, it is important to acknowledge that this project relies on data-driven analysis. However, our collected road network data for Turkey is incomplete, particularly in urban areas where a significant number of roads are missing. Therefore, generating a more granular and dense road network dataset becomes imperative to gain a comprehensive understanding of the connectivity of Turkey's transportation network.

Next, it should be noted that the lack of available earthquake data specifically indicating which roads have withstood seismic events in Turkey prevents us from validating our model. To address this limitation, it would be valuable to establish communication with Turkish authorities or develop a satellite imagery-based model that can identify damaged or broken roads, thus facilitating the validation of our approach. The NASA Disasters Program (ARIA, Copernicus, Sentinel-1) generated a damage map of a subregion in Turkey, including the cities of Iskenderun, Antakya and Kahramanmaraş. This map was derived from synthetic aperture radar (SAR) images on Feb. 10, 2023 by the Copernicus Sentinel-1 satellites operated by the European Space Agency (ESA). Damage values range from 0 to 255, with the color variation on their map from yellow to red indicating increasingly more significant surface change/damage. However this damage proxy map may be less reliable over vegetated areas and therefore not a adequate testing set.

Moreover, our project relies on a predictive model to estimate the probability of road breakage. Developing an accurate model adding on factors such as road type, road year of construction, infrastructure damage susceptible to block road access, local temperature, soil composition and other relevant features capable of predicting road damage or preservation will greatly enhance the overall quality of our methodology.

Lastly, it is important to highlight that our methodology is not limited to a specific geographic region. Consequently, it can be applied to earthquake sequences occurring worldwide. Therefore, extending this technology to analyze the road networks of other regions such as Chile, Japan, or California is both feasible and advantageous.

6. Conclusion

To summarize, in this project, we introduced a methodology for simulating the impact of consecutive earthquakes on transportation networks and evaluating their resilience. Our approach enabled us to identify vulnerable zones in Turkey, while also being applicable to other regions. Furthermore,

we proposed suitable locations for emergency centers within these at-risk zones, which could potentially face isolation following a natural disaster. Moving forward, several future directions for this project are anticipated, including expanding the dataset, validating the model, and extending its application to regions such as California, Chile, or Japan.

References

- United States Geological Survey. <https://earthquake.usgs.gov/earthquakes/map/?currentFeatureId=us6000jqcn&extent=18.81272,12.78809&extent=48.07808,65.1709&range=search&sort=largest&showPopulationDensity=true&search=%7B%22name%22:%22Search%20Results%22,%22params%22:%7B%22starttime%22:%222023-02-01%2000:00:00%22,%22endtime%22:%222023-03-01%2023:59:59%22,%22maxlatitude%22:38.051,%22minlatitude%22:35.482,%22maxlongitude%22:42.363,%22minlongitude%22:35.244,%22minmagnitude%22:2.5,%22orderby%22:%22magnitude%22%7D%7D>. [Accessed April 4th, 2023].
- Anbazhagan, P., Srinivas, S., and Chandran, D. Classification of road damage due to earthquakes. *Natural hazards*, 60:425–460, 2012.
- Ball, M. O., Colbourn, C. J., and Provan, J. S. Chapter 11 network reliability. In *Network Models*, volume 7 of *Handbooks in Operations Research and Management Science*, pp. 673–762. Elsevier, 1995.
- Humanitarian Data Exchange. Roads in Turkey. <https://data.humdata.org/dataset/roads-in-turkey>. [Accessed April 4th, 2023].
- Kilanitis, I. and Sextos, A. Impact of earthquake-induced bridge damage and time evolving traffic demand on the road network resilience. *Journal of traffic and transportation engineering (English edition)*, 6(1):35–48, 2019.
- Li, D., Zhang, Q., Zio, E., Havlin, S., and Kang, R. Network reliability analysis based on percolation theory. *Reliability Engineering & System Safety*, 142:556–562, 2015.
- Murtagh, F. and Contreras, P. Algorithms for hierarchical clustering: an overview. *Wiley Interdisciplinary Reviews: Data Mining and Knowledge Discovery*, 2(1):86–97, 2012.
- NASA Disasters Mapping Portal. Disaster Data Mapping and Visualization. <https://maps.disasters.nasa.gov/arcgis/home/item.html?id=bd10c68dc2714258919c9bec4a4f3d02>. [Accessed April 4th, 2023].
- Schaeffer, S. E. Graph clustering. *Computer science review*, 1(1):27–64, 2007.
- Sextos, A., Kilanitis, I., Kyriakou, K., and Kappos, A. Resilience of road networks to earthquakes. In *16th world conference on earthquake engineering*, pp. 9–13, 2017.
- SimpleMaps. TR Cities. <https://simplemaps.com/data/tr-cities>. [Accessed April 4th, 2023].
- Sun, Y.-R., Zhou, W.-Y., et al. An inclusion-exclusion algorithm for network reliability with minimal cut sets. *American Journal of Computational Mathematics*, 2(4):316–320, 2012.